Accepted Manuscript

Characterisation of *Anopheles gambiae* heme oxygenase and metalloporphyrin feeding suggests a potential role in reproduction

Christopher S. Spencer, Cristina Yunta, Glauber Pacelli Gomes de Lima, Kay Hemmings, Lu-Yun Lian, Gareth Lycett, Mark J.I. Paine

PII: S0965-1748(18)30037-7

DOI: 10.1016/j.ibmb.2018.04.010

Reference: IB 3055

To appear in: *Insect Biochemistry and Molecular Biology*

Received Date: 31 January 2018

Revised Date: 23 March 2018

Accepted Date: 29 April 2018

Please cite this article as: Spencer, C.S., Yunta, C., Gomes de Lima, G.P., Hemmings, K., Lian, L.-Y., Lycett, G., Paine, M.J.I., Characterisation of *Anopheles gambiae* heme oxygenase and metalloporphyrin feeding suggests a potential role in reproduction, *Insect Biochemistry and Molecular Biology* (2018), doi: 10.1016/j.ibmb.2018.04.010.

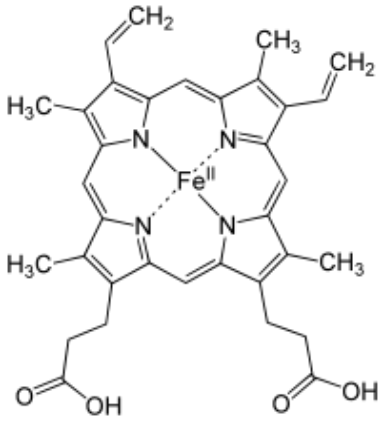

heme

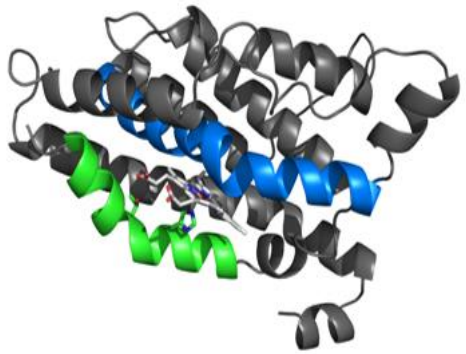

***Anopheles gambiae* heme oxygenase**

cytochrome P450 reductase
O_2
NADPH

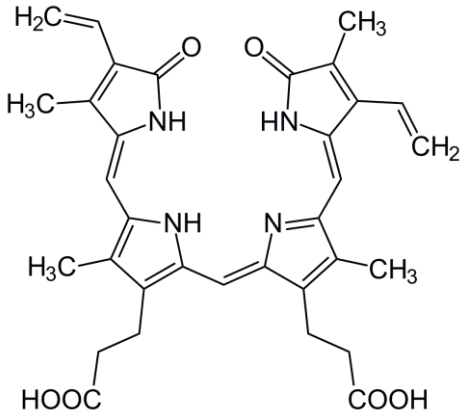

biliverdin
Fe^{2+}
CO

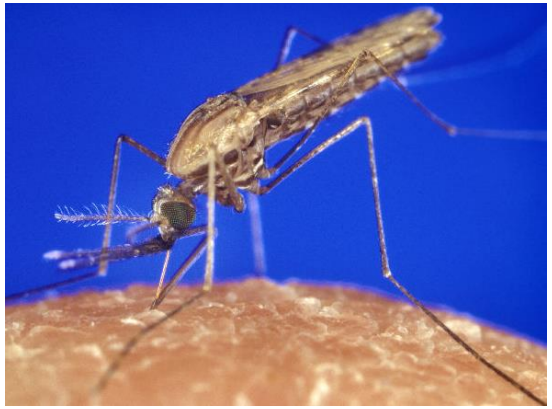

SnPP, ZnPP

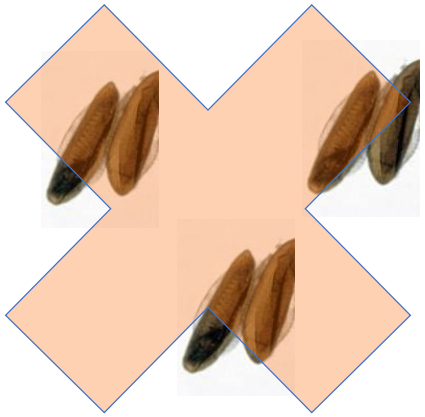

Oviposition inhibition

Characterisation of *Anopheles gambiae* heme oxygenase and metalloporphyrin feeding suggests a potential role in reproduction

Short title: Characterisation of AgHO

Christopher S. Spencer [1], Cristina Yunta [1], Glauber Pacelli Gomes de Lima [1], Kay Hemmings [1], Lu-Yun Lian [2], Gareth Lycett [1], Mark J. I. Paine [1,*]

[1] Liverpool School of Tropical Medicine, Liverpool, L3 5QA, UK

[2] Institute of Integrative Biology, University of Liverpool, Liverpool, UK

* Corresponding author, E-mail: mark.paine@lstmed.ac.uk

Abstract

The mosquito *Anopheles gambiae* is the principal vector for malaria in sub-Saharan Africa. The ability of *A. gambiae* to transmit malaria is strictly related to blood feeding and digestion, which releases nutrients for oogenesis, as well as substantial amounts of highly toxic free heme. Heme degradation by heme oxygenase (HO) is a common protective mechanism, and a gene for HO exists in the *An. gambiae* genome HO (AgHO), although it has yet to be functionally examined. Here, we have cloned and expressed *An. gambiae* HO (AgHO) in *E. coli*. Purified recombinant AgHO bound hemin stoichiometrically to form a hemin–enzyme complex similar to other HOs, with a K_D of 3.9 ± 0.6 μM; comparable to mammalian and bacterial HOs, but 7-fold lower than that of *Drosophila melanogaster* HO. AgHO also degraded hemin to biliverdin and released CO and iron in the presence of NADPH cytochrome P450 oxidoreductase (CPR). Optimal AgHO activity was observed at 27.5^{o}C and pH 7.5. To investigate effects of AgHO inhibition, adult female *A. gambiae* were fed heme analogues Sn- and Zn-protoporphyrins (SnPP and ZnPP), known to inhibit HO. These led to a dose dependent decrease in oviposition.

Cu-protoporphyrin (CuPP), which does not inhibit HO had no effect. These results demonstrate that AgHO is a catalytically active HO and that it may play a key role in egg production in mosquitoes. It also presents a potential target for the development of compounds aimed at sterilising mosquitoes for vector control.

Keywords

mosquito, insecticide, malaria, insect vectors, metabolism, hematophagy, reproduction, protoporphyrin, oviposition

1. Introduction

The mosquito *Anopheles gambiae* is the principal vector for malaria in sub-Saharan Africa, a disease that affects over 200 million people (WHO, 2015). Insecticides coated on bednets or sprayed on walls remain the most widely used and effective means to block the spread of disease (Bhatt et al., 2015). However, resistance exists to most of the classes of insecticides available for adult mosquito control (pyrethroids, organophosphates, carbamates and DDT) and new targets for the design of reagents to prevent transmission are urgently needed (Hemingway et al., 2006). The malarial parasite is transmitted during hematophagy by female mosquitoes that require blood for egg production. Blood contains large quantities of heme, of which only a small fraction (13%) is incorporated into adult tissues and developing embryos (Braz et al., 2001; Zhou et al., 2007) presumably as a prosthetic group in hemoproteins such as nitric oxide synthase (Yuda et al., 1996), catalase (Paes et al., 2001) and the cytochromes P450 (Ranson et al., 2002; Tijet et al., 2001). However, excess heme is highly toxic generating reactive oxygen species (Gutteridge and Smith, 1988) that can lead to oxidation of lipids (Tappel, 1955), degradation of proteins (Aft and Mueller, 1984), scission of DNA (Aft and Mueller, 1983) and physical disruption of phospholipid membranes (Schmitt et al., 1993). Hematophagous insects have evolved numerous protective mechanisms to minimise heme mediated toxicity, such as hemozoin formation (Oliveira et al., 1999), use of anti-oxidants, heme binding proteins (Maya-

Monteiro et al., 2000; Oliveira et al., 1995) and enzymatic heme degradation (Paiva-Silva et al., 2006). These offer potentially new targets to disrupt hemostasis for insecticide design.

Heme degradation by heme oxygenase (HO) has been described in several organisms, including mammals (Wang et al., 1997; Wilks and de Montellano, 1993), plants (Muramoto et al., 1999), bacteria (Wilks and Schmitt, 1998; Zhu et al., 2000) and insects (Zhang et al., 2004). The canonical reaction catalysed by mammalian heme oxygenase (HO, EC 1.14.99.3) results in the release of ferrous ion (Fe^{2+}) and the formation of carbon monoxide (CO) and green biliverdin (BV) IXα (Tenhunen et al., 1968). In addition to heme detoxification, the reaction products may potentially play other key physiological roles. The green coloured BV and the reduced yellow bilirubin product have antioxidant properties capable of scavenging peroxyl radicals (Stocker et al., 1987), while CO can act as a signalling molecule with potential regulatory roles in blood pressure (Stec et al., 2008), inflammation (Otterbein et al., 2000) and apoptosis (Soares et al., 2002).

In hematophagous insects heme degradation is poorly understood, yet may be important for blood meal tolerance or other aspects of a blood feeding habit. Examination of heme-degradation products in blood sucking insect species suggests there may be significant differences with canonical HO activity. For example, the kissing bug *Rhodnius prolixus* follows a complex pathway involving amino-acid conjugation that results in dicysteinyl-BV IX as the end product of heme degradation, whereas biglutaminyl-BV IX-α is the end product in *Aedes aegypti* (Paiva-Silva et al., 2006; Pereira et al., 2007). *Ae. aegypti* and *R. prolixus* contain putative HO genes (Accession numbers AAEL008136 and RPRC006832 respectively) consistent with the involvement of heme oxygenase in heme degradation pathways (Paiva-Silva et al., 2006; Pereira et al., 2007), although these have yet to be characterised; to date, *Drosophila melanogaster* HO is the only insect HO to have been cloned and characterised (Zhang et al., 2004).

Here, we describe the cloning and characterisation of *An. gambiae* HO (AgHO). The work confirms the enzyme has HO activity, while inhibition of AgHO in adult female *An. gambiae* indicates a role in egg production that provides insight on HO activity in blood feeding insects and potential new sterilising targets for insecticide development.

2. Materials and Methods

2.1 Reagents

Chemicals were obtained from Sigma-Aldrich unless otherwise indicated. Enzymes for DNA manipulation were supplied by New England Biolabs. Protoporphyrin inhibitors were provided by Tocris Bioscience. Plasmids and competent *E. coli* cells were obtained from Life Technologies. MdCPR was provided by Evangelia Morou (University of Crete), HsCPR was obtained from Sigma-Aldrich, and AgCPR was produced as previously described (Lian et al., 2011).

2.2 Construction of AgHO expression plasmids

The putative AgHO gene, AGAP003975 was identified by querying the genome database VectorBase for the words “heme oxygenase.” The gene is located on the 2R chromosome, and contains a single intron. The full length AgHO coding sequence was amplified by PCR using Phusion DNA polymerase (New England Biolabs) from *An. gambiae* cDNA (Stevenson et al., 2011) using forward primer pJETF (5’-GAGACAT**ATG**GCACAAAATGTGCCTTTTTCG-3’), containing the ATG start (bold) and an NdeI site (underlined) and reverse primer pJETR (5’-AAGCTT**TCA**CAACGTTTGCTCTT
GCTCGTG-3’), encoding the stop codon (TGA) followed by a Hind III site (underlined). The 0.75-kb PCR product was cloned into the pJET1.2 (Invitrogen) to generate pJET-AgHO, and sequenced for verification. The coding sequence matched the VectorBase reference sequence

(AGAP003975). The coding sequence was synthesized, and codon optimised for expression in *E. coli* (LifeTechnologies). The coding sequence was cloned into pMK holding vector with 5' NdeI and NcoI restriction sites and 3' BamHI, EcoRI, HindIII and KpnI added for compatibility with pCold-II and other expression vectors. The AgHO coding sequence was excised by NdeI and EcoRI digestion and sub-cloned into NdeI/EcoRI digested pCold-II.

2.3 Expression and purification of AgHO

Competent *E. coli* BL-21* cells were transformed with pCold-IIAgHO. A single transformed colony was precultured in 10 mL Terrific Broth containing ampicillin (100µg mL^{-1}) at 37^{o}C overnight with shaking at 180rpm. The 10mL culture was then used to inoculate 1L of the same medium held in a 2L Erlenmeyer flask. The culture was incubated at 37 ^{o}C, shaking at 180 rpm until the A_{600} reached 0.3-0.5, at which point the temperature was reduced to 16 ^{o}C, and shaking reduced to 160 rpm. Once the A_{600} reached 0.7, the culture was induced by addition of IPTG to a final concentration of 0.5 mM. The culture was incubated for another 48h. Bacteria were harvested by centrifugation at 8000rpm for 10 minutes. The bacterial pellet was placed on ice and resuspended in 25mL ice cold lysis buffer (150mM NaCl, 50mM Tris pH 8.0, 50mM imidazole, 0.5% Triton X100). Once resuspended, phenylmethylsulfonyl fluoride (PMSF) was added to a final concentration of 1mM. The pellet was lysed with lysozyme (final concentration 0.2 mg mL^{-1}) then briefly sonicated on ice before centrifugation at 30000*g* for 25 minutes. The resulting supernatant was used for purification.

A Ni-NTA column was pre-equilibrated with wash buffer (150mM NaCl, 50mM Tris pH 8.0, 50mM imidazole, 0.1% Triton X100). The supernatant was filtered through a 0.5-micron filter before being applied to the Ni-NTA column. 10mL wash buffer was used to rinse the resin, and 10mL elution buffer (150mM NaCl, 50mM Tris pH 8.0, 400mM imidazole, 0.1% Triton X100) was used to elute the AgHO from the column. Fractions containing AgHO were pooled and dialysed overnight against ice cold TS (50mM Tris pH 8.0, 150mM NaCl).

Hemin was added to the purified AgHO to give a final 2:1 heme: protein ratio. The sample was applied to a PD Minitrap G-25 column pre-equilibrated with TS. The flow through was discarded and the protein eluted in TS.

2.4 Absorption spectroscopy and heme binding

The ferrous-CO complex was formed by the addition of dithionite to a carbon monoxide-saturated solution of the ferric heme-AgHO complex. The ferrous CO-heme-AgHO complex was passed through Sephadex G-25 to remove the excess reductant and generate the ferrous oxyheme-AgHO complex. The absorbance between 350 and 750 nm was measured on a Cary 4000 absorption spectrophotometer.

Heme binding of AgHO was measured by titrating hemin to 10 μM AgHO in 90μL TS. The reference cuvette contained 90μL TS without enzyme. A solution of 50 μM hemin was titrated in 2 μL aliquots to test and reference cuvettes at 25 ^{o}C with 5 min equilibration between additions. The absorbance range 350 and 750 nm was measured on a Cary 4000 absorption spectrophotometer. K_D was calculated using a one-site binding model.

2.5 Identification of biliverdin as an AgHO reaction product

The reaction mixture (100μL solution, 10μM AgHO-heme complex, 3μM CPR, 300μM NADPH in a buffer of 150mM NaCl, 50mM Tris, pH 7.4, 0.1% Triton x100) was placed in a 90μL quartz cuvette. The reference cuvette contained only buffer and CPR. The reaction was initiated with addition of NADPH, and absorbance from 750nm to 350nm was immediately measured. Absorbance was measured every ten minutes for two hours. Negative controls lacking NADPH, CPR and AgHO were used to ensure that heme degradation was not spontaneous, non-enzymatic or CPR driven.

2.6 Identification of CO as an AgHO reaction product

The final reaction mixture was 100µL containing 10µM AgHO-heme complex, 3µM AgCPR, 300µM NADPH, 150µM myoglobin in a buffer of 150mM NaCl, 50mM Tris, pH 7.4, 0.1% Triton x100. All components except for myoglobin and NADPH were placed in in a 90µL quartz cuvette, and then blanked. The reference cuvette contained only buffer and CPR. Myoglobin was added to the sample cuvette, the reaction was initiated with addition of NADPH, and absorbance from 600nm to 350nm was measured immediately then every ten minutes for two hours. Negative controls were used that omitted each one of NADPH, CPR, and AgHO.

2.7 Identification of ferrous iron as an AgHO reaction product

The reaction mixture (100µL solution, 10µM AgHO-heme complex, 3µM AgCPR, 250µM ferrozine, 300µM NADPH in a buffer of 150mM NaCl, 50mM Tris, pH 7.4, 0.1% Triton x100) was placed in a 90µL quartz cuvette. The reference cuvette contained only buffer and CPR. The reaction was initiated with addition of NADPH, and absorbance from 750nm to 350nm was immediately measured. Absorbance was measured every ten minutes for one hour. Control systems omitted, in turn, NADPH, CPR, and AgHO.

2.8 AgHO pH experiments

Each reaction mixture (200µL solution, 10µM AgHO-heme complex, 3µM AgCPR, 250µM Ferrozine, 300µM NADPH in a buffer of 150mM NaCl, 50mM Tris, 0.1% Triton x100) was placed in a well in a Nunc 96-well plate. There were six different pHs for the 50mM Tris buffer; 6.5, 7.0, 7.5, 8.0, 8.5, 9.0. Four reaction wells were set up for each buffer – three experimental wells and one control well. The reaction was initiated with addition of NADPH, the control wells had buffer added rather than NADPH. Absorption at 562nm was measured every 15 seconds for 5 minutes.

2.9 AgHO temperature experiments

Each reaction mixture (200µL solution, 10µM AgHO-heme complex, 3µM AgCPR, 250µM Ferrozine, 300µM NADPH in a buffer of 150mM NaCl, 50mM Tris pH 7.4, 0.1% Triton x100) was placed in a well in a Nunc 96-well plate. Four reaction wells were set up– three experimental wells and one control well. The spectrophotometer was set to 20^{o}C, then the plate was introduced and allowed to equilibrate to the correct temperature for five minutes. The reaction was initiated with addition of NADPH, the control wells had buffer added rather than NADPH. Absorption at 562nm was measured every 15 seconds for 5 minutes. The experiment was repeated at 25^{o}C, 27.5^{o}C, 30^{o}C, 32.5^{o}C, 35^{o}C, 37.5^{o}C and 40^{o}C.

2.10 *In vivo* AgHO inhibition assays

An. gambiae mosquitoes of the *Tiassale* strain (MRA-762) were maintained at 26 °C, 80% relative humidity and a 12:12 hours light: dark cycle. Larvae were fed with finely ground fish food (TetraMin). Adult mosquitoes were provided with 10% sucrose solution *ad libitum* and given human blood through a membrane feeder to stimulate egg laying.

10mM protoporphyrin (SnPP, ZnPP, CuPP) stocks were made by dissolving the protoporphyrins in 50mM NaOH. The protoporphyrins were added to blood in a volume of no more than 200µL in 5mL heparinized human blood. Final concentrations of protoporphyrin in blood were 0µM, 40µM, 100µM and 400µM.

Cohorts of *An. gambiae* mosquitoes, were fed the inhibitor-supplemented blood *via* hemotek bloodfeeders, for two hours, in darkness. Mosquitoes were visually confirmed to have fed. Those individuals that had not fed were excluded. 25 individuals from each feeding group were isolated and kept under standard conditions and fed 10% sucrose *ad libitum*. After two days, an egg paper was introduced to allow mosquitoes to lay. After two further days, the egg paper was removed, and laid eggs were counted.

2.11 Data analysis

Binding models, statistical analysis and graphs were generated using GraphPad Prism version 7.00 for Windows, GraphPad Software, La Jolla California USA, www.graphpad.com. Sequence analysis was performed using T-Coffee (Notredame et al., 2000).

3. Results

3.1 AgHO sequence analysis

An. gambiae HO was initially cloned from cDNA and sequence analysis revealed no nucleotide differences compared with the genome sequence (accession number: AGAP003975 (Giraldo-Calderón et al., 2014; Holt et al., 2002)). The 750 nucleotide AgHO coding sequence encodes a 249 amino acid protein with a molecular weight of 29.5kDa. Comparison of AgHO with mammalian, bacterial and insect (hematophagous and non-hematophagous) are shown in Figure 1 (Notredame et al., 2000). The proximal ligand of prototypical human HO-1, His-25, is present in AgHO (His-19), suggesting a conserved role for this residue in heme binding (Schuller et al., 1999). Similarly, there is conservation in AgHO residues Thr-15, Asp-23, and Phe-199 associated with proximal heme binding in HO-1 (Thr-21, Glu-29, and Phe-207) (Schuller et al., 1999). HO-1 residues Gly-139, Gly-143, and Leu-147 associated with flexing the distal helix for active site opening and closing are also conserved in AgHO; Glu-123, Glu-128, Leu-131. However, HO-1 residues Met-34 and Phe-37 that interact with α-meso edge of heme are diverged in AgHO (Ala-31 and Leu-34) and other insect HOs.

3.2 Functional expression in E. coli

The full length AgHO sequence was codon optimised for *E. coli* expression and cloned into pCold II for AgHO production. Interestingly, the colonies and cultures were not observed to have a green tint as has been observed in other HO expression systems (Wilks and Schmitt, 1998;

Zhu et al., 2000). Maximal yields of AgHO were obtained 48 hr post-induction. The his-tagged protein was purified via Ni-NTA purification, with a yield of ~5mg AgHO per litre of cell culture. Purity was estimated at >95% based on the presence of a single band of the expected size for AgHO (29.5kDa) measured by SDS-PAGE (Figure 2).

3.3 Properties of the heme-AgHO complex

AgHO was incubated with heme and unbound heme removed by Sephadex G-25 size exclusion chromatography. All HOs characterised thus far have been found to bind heme stoichiometrically, forming stable complexes with characteristic absorption spectra. The Soret maximum of the heme-AgHO complex was 398 nm (Figure 3). The CO-reduced heme-HO complex produced a typical ferric heme spectrum with a Soret band at 412 nm and α/β bands at 564 and 535 nm, respectively (Figure 3). Following passage of the ferrous carbon monoxide complex over Sephadex G-25, the Soret band shifts from 412 to 400 nm and the α/β bands to 571 and 540 nm indicative of the formation of a ferrous dioxygen complex (Figure 3). These values are comparable to those reported for the corresponding complex of human (0.84 ± 0.2 μM) and *C. diptheriae* (2.5 ± 1 μM) heme oxygenases (Wilks et al., 1996; Wilks and Schmitt, 1998). The extinction coefficient of the AgHO-heme complex at 398nm (ε_{398}) was calculated to be 105.73mM^{-1} cm^{-1} (Bar, 2015; Berry and Trumpower, 1987).

The stoichiometry of heme bound to AgHO was calculated by difference absorption spectroscopy (Figure 4). Titration of AgHO with heme produced a K_D of 3.9 ± 0.6 μM, with 1:1 heme: AgHO stoichiometry obtained at saturation. The AgHO K_D value for heme was thus intermediate between the 27 ± 3 μM reported for *D. melanogaster* (Zhang et al., 2004) and 0.84 ± 0.2 μM recorded for human HO (Wilks et al., 1996).

3.4 AgHO catalytic activity

Biliverdin production. Oxidation of heme by HO results in the production of biliverdin, which can be followed by shifts in absorption spectra (Wilks et al., 1995; Wilks and de Montellano, 1993; Wilks and Schmitt, 1998). HO activity requires electrons, which are donated *in vivo* by NADPH via coupled interactions with membrane anchored CPR. To examine AgHO in vitro activity, this reaction was assayed with three alternative CPR sources. It is typical for HO reactions to be studied by examination of bilirubin formation as part of a biliverdin reductase-coupled reaction, however insects have no biliverdin reductase, so HO activity was examined by directly measuring reductions in the typical heme peaks at 398mm, 603nm and 579nm. Incubation with truncated AgCPR (Figure 5A) lacking the amino-terminal membrane anchor gave evidence of heme oxidation from a reduction of the Soret peak, however, enzyme activity was relatively weak, compared with reactions with full length house-fly (MdCPR, Figure 5B) and human CPRs (hCPR, Figure 5C), presumably due to the lack of membrane anchor. However, all reactions produced a reduction in the heme Soret and α/β peaks peak (398nm, 603nm and 579nm respectively), indicative of heme catabolism. The appearance of a broad absorption peak centred at 680nm was also evident, corresponding with peak absorption for biliverdin. Control reactions lacking CPR or NADPH showed no reduction in Soret or α/β peak absorption or increase at 680nm.

CO production. In order to measure the production of CO, myoglobin was included with AgHO catalysed heme oxidation reactions. Myoglobin is a hemoprotein that allows CO released by AgHO to be detected by spectral shifts of myoglobin following CO binding (Figure 6) (Wilks and Schmitt, 1998); there was a clear myoglobin Soret peak shift to a higher wavelength (414 nm) with a concurrent increase in α/β peak absorption. These results are characteristic of CO binding and indicative of CO generation by AgHO. Soret peak shifts were not observed in negative controls that lacked NADPH or AgCPR.

Ferrous iron (Fe^{2+}) production. To measure ferrous iron (Fe^{2+}) production, ferrozine was added to AgHO–heme reactions (Soldano et al., 2014). The release of Fe^{2+} was measured by the formation of the magenta ferrozine - metal ion complex (562 nm). As illustrated in Figure 7, degradation of heme by AgHO resulted in the production of a broad peak centred at 562nm, (in a time dependent manner see inset Figure 7) characteristic of the formation of a ferrozine - metal ion complex following AgHO mediated heme catabolism.

Effect of pH and temperature on AgHO activity. The effect of pH on AgHO activity was measured in the range 6.5 - 9. Enzyme activity peaked at pH 7.5, consistent with standard physiological conditions (Figure 8A). Enzyme activity was markedly reduced at pH 9 possibly due to inhibition of AgHO binding to heme *via* heme propionate groups, or due to denaturation of the functional conformation of AgHO. When testing different temperatures (Figure 8B), highest activity was measured at 27.5^{o}C, with activity minimal at 20^{o}C. This is optimal temperature for mosquito rearing.

3.5 Inhibition of AgHO activity in *An. gambiae*.

Heme analogues zinc protoporphyrin (ZnPP) and tin protoporphyrin (SnPP) are well known to competitively inhibit HO activity (Caiaffa et al., 2010; Maines, 1981). Previous work with *R. prolixus* has shown that inhibition of HO activity by SnPP results in inhibition of oviposition, suggesting that the HO pathway plays a role in fecundity (Caiaffa et al., 2010). Similarly, we examined the effects on egg production in *An. gambiae*. Mosquito cohorts were fed on human blood dosed with varying concentrations of ZnPP and SnPP. The cohorts were then given time to lay eggs, and the eggs laid were counted. Copper protoporphyrin (CuPP), a heme analogue that does not inhibit HO (Drummond and Kappas, 1981), was employed as a negative control. Both SnPP and ZnPP inhibited oviposition in a dose dependent manner (Figures 9A, B). SnPP was the most potent inhibitor in line with previous mammalian studies (Drummond and Kappas, 1981). Addition of CuPP to mosquito bloodmeals (Figure 9C) had minimal effect on fecundity.

CuPP is useful as a control, as it has been shown to have similar effects to SnPP and ZnPP on non-HO proteins, such as guanylyl cyclase (Ignarro et al., 1984). Though mortality rates were not formally tested, approximately ten percent of mosquitoes died per cohort, which was independent of the type and concentration of the inhibitor applied, suggesting that there was minimal effect on mortality in the time frame of the experiment.

4. Discussion

The ability of *An. gambiae* to transmit malaria is dependent on blood feeding by females, which provides nutrients for egg production, as well as substantial amounts of cytotoxic heme. HO enzymes are widely expressed by organisms and heme degradation pathways have been described in the mosquito *Ae. aegypti* and the blood sucking hemipteran, *R. prolixus* (Paiva-Silva et al., 2006; Pereira et al., 2007). Having expressed and purified AgHO, we have been able to demonstrate *in vitro* that AgHO binds heme with 1:1 stoichiometry and has heme oxygenase activity, producing biliverdin, carbon monoxide and ferrous iron. AgHO activity was optimal in the physiological range of pH and temperature i.e. pH 7.5 and 27.5 ^{o}C. The latter corresponds to the behaviour of blood fed mosquitoes that seek temperatures in the range of 26-28^{o}C at which to rest (Blanford et al., 2009). While analysis of the *in vivo* reaction products is required, the strong sequence homology with *Ae. aegypti* (62% identity) suggests that the cognate HO substrate. is most likely to be heme rather than a heme conjugate as in *Rhodnius*. AgHO contains H19 at a conserved position on the proximal heme face that is expected to coordinate heme with T15 *via* a water molecule. The K_D of AgHO was estimated to be 3.9 μM using a one-site binding model. This value is seven-fold lower than DmΔHO (27 μM) (Zhang et al., 2004), the only other insect HO characterised. Unlike human and many other HOs that generate biliverdin IXα, hemin catabolism by DmΔHO is not α-specific and yields three isomers of biliverdin, IXα, IXβ, and IXδ. Thus, heme binding differences may be indicative of potential structural differences in the heme binding pocket between the two enzymes, possibly relating to the accommodation of native or conjugated heme substrates. This might explain the divergence

of human HO-1 residues Met-34 and Phe-37 that interact with α-meso edge of heme in the equivalent positions in AgHO (Ala-31 and Leu-34) and other insect HOs (Figure 1).

Although AgHO might be expected to play a key role in heme degradation and detoxification, extremely large amounts of cytotoxic heme are released following a blood meal, requiring multiple protective mechanisms (Giraldo-Calderón et al., 2014; Otterbein et al., 2000). Sequestration through the formation of heme aggregates such as hemozoin is considered a primary route of heme detoxification in hematophagous organisms (Lara et al., 2005; Oliveira et al., 2005; Otterbein et al., 2000; Toh et al., 2010), thus AgHO likely plays a role in the degradation of the blood heme fraction that escapes heme aggregation. HO may play other roles, however; for instance, in *D. melanogaster*, DmHO appears to play a role in tissue development (Cui et al., 2008) and regulation of circadian rhythms (Klemz et al., 2017). Mice lacking HO-1 have impaired production of oocytes (Zenclussen et al., 2012) and there is accruing evidence that mammalian HO plays an important role in the female reproductive system, potentially through the influence of CO production on the regulation of metabolic pathways (Němeček et al., 2017). In insects, inhibition of HO activity in SnPP fed *R. prolixus* led to reduced oviposition along with increased lipid peroxidation in the midgut and reduction in hemozoin formation (Caiaffa et al., 2010). Most recently, silencing of RpHO has been shown to have a deleterious effect on oviposition and egg viability (Walter-Nuno et al., 2018), providing compelling evidence for a reproductive role for HO in insects. AgHO gene expression is reported to be significantly increased in the ovaries of blood-fed female *An. gambiae* (Marinotti et al., 2005), and our results show that egg laying by *An. gambiae* is dramatically reduced following consumption of the heme oxygenase inhibitors SnPP and ZnPP. Importantly, we cannot rule out off-target effects of heme analogues that may contribute to the reduction in egg laying. Thus, further genetic knockdown studies are required to confirm the role of AgHO in reproduction.

In the context of malaria control, although the AgHO inhibition experiments produced no obvious effects on mortality, disruption of oviposition could have a sterilizing effect in reducing or eliminating insect populations. At present, the sterilising effect of pyriproxyfen on adult female *An. gambiae* is being trialled for use in bednets as a new intervention for malaria control (Ngufor et al., 2014), while the mass release of genetically engineered sterile male *Ae. aegypti* has proved successful in the suppression of field populations of the mosquito vector of dengue and zika viruses (Carvalho et al., 2015; Harris et al., 2012). Thus, the physiological adaptations in mosquitoes that mitigate heme toxicity such as heme degradation offer potential new targets for vector control.

Funding and Acknowledgements

This work was funded by the Leverhulme Trust and in part by Conselho Nacional de Densenvolvimento Científico e Technológico (CNPq). We thank Evangelia Morou for the gift of MdCPR.

References

Aft, R.L., Mueller, G.C., 1983. Hemin-mediated DNA strand scission. Journal of Biological Chemistry 258, 2069-2072.

Aft, R.L., Mueller, G.C., 1984. Hemin-mediated oxidative-degradation of proteins. Journal of Biological Chemistry 259, 301-305.

Bar, I.G., F., 2015. Pyridine Hemochromagen Assay for Determining the Concentration of Heme in Purified Protein Solutions. Bio-Protocol 5, e1594.

Berry, E.A., Trumpower, B.L., 1987. Simultaneous determination of hemes a, b, and c from pyridine hemochrome spectra. Analytical Biochemistry 161, 1-15.

Bhatt, S., Weiss, D.J., Cameron, E., Bisanzio, D., Mappin, B., Dalrymple, U., Battle, K.E., Moyes, C.L., Henry, A., Eckhoff, P.A., 2015. The effect of malaria control on Plasmodium falciparum in Africa between 2000 and 2015. Nature 526, 207-211.

404 Blanford, S., Read, A.F., Thomas, M.B., 2009. Thermal behaviour of Anopheles stephensi in response to
405 infection with malaria and fungal entomopathogens. Malar J 8.
406 Braz, G.R.C., Abreu, L., Masuda, H., Oliveira, P.L., 2001. Heme biosynthesis and oogenesis in the blood-
407 sucking bug, Rhodnius prolixus. Insect Biochemistry and Molecular Biology 31, 359-364.
408 Caiaffa, C.D., Stiebler, R., Oliveira, M.F., Lara, F.A., Paiva-Silva, G.O., Oliveira, P.L., 2010. Sn-
409 protoporphyrin inhibits both heme degradation and hemozoin formation in Rhodnius prolixus midgut.
410 Insect Biochemistry and Molecular Biology 40, 855-860.
411 Carvalho, D.O., McKemey, A.R., Garziera, L., Lacroix, R., Donnelly, C.A., Alphey, L., Malavasi, A.,
412 Capurro, M.L., 2015. Suppression of a field population of Aedes aegypti in Brazil by sustained release of
413 transgenic male mosquitoes. PLoS neglected tropical diseases 9, e0003864.
414 Cui, L., Yoshioka, Y., Suyari, O., Kohno, Y., Zhang, X., Adachi, Y., Ikehara, S., Yoshida, T.,
415 Yamaguchi, M., Taketani, S., 2008. Relevant expression of Drosophila heme oxygenase is necessary for
416 the normal development of insect tissues. Biochemical and Biophysical Research Communications 377,
417 1156-1161.
418 Drummond, G.S., Kappas, A., 1981. Prevention of neonatal hyperbilirubinemia by tin protoporphyrin IX,
419 a potent competitive inhibitor of heme oxidation. Proceedings of the National Academy of Sciences 78,
420 6466-6470.
421 Giraldo-Calderón, G.I., Emrich, S.J., MacCallum, R.M., Maslen, G., Dialynas, E., Topalis, P., Ho, N.,
422 Gesing, S., Consortium, V., Madey, G., 2014. VectorBase: an updated bioinformatics resource for
423 invertebrate vectors and other organisms related with human diseases. Nucleic acids research 43, D707-
424 D713.
425 Gutteridge, J.M., Smith, A., 1988. Antioxidant protection by haemopexin of haem-stimulated lipid
426 peroxidation. Biochem J 256, 861-865.
427 Harris, A.F., McKemey, A.R., Nimmo, D., Curtis, Z., Black, I., Morgan, S.A., Oviedo, M.N., Lacroix, R.,
428 Naish, N., Morrison, N.I., 2012. Successful suppression of a field mosquito population by sustained
429 release of engineered male mosquitoes. Nature biotechnology 30, 828-830.

Hemingway, J., Beaty, B.J., Rowland, M., Scott, T.W., Sharp, B.L., 2006. The Innovative Vector Control Consortium: improved control of mosquito-borne diseases. Trends in Parasitology 22, 308-312.

Holt, R.A., Subramanian, G.M., Halpern, A., Sutton, G.G., Charlab, R., Nusskern, D.R., Wincker, P., Clark, A.G., Ribeiro, J.M.C., Wides, R., Salzberg, S.L., Loftus, B., Yandell, M., Majoros, W.H., Rusch, D.B., Lai, Z.W., Kraft, C.L., Abril, J.F., Anthouard, V., Arensburger, P., Atkinson, P.W., Baden, H., de Berardinis, V., Baldwin, D., Benes, V., Biedler, J., Blass, C., Bolanos, R., Boscus, D., Barnstead, M., Cai, S., Center, A., Chatuverdi, K., Christophides, G.K., Chrystal, M.A., Clamp, M., Cravchik, A., Curwen, V., Dana, A., Delcher, A., Dew, I., Evans, C.A., Flanigan, M., Grundschober-Freimoser, A., Friedli, L., Gu, Z.P., Guan, P., Guigo, R., Hillenmeyer, M.E., Hladun, S.L., Hogan, J.R., Hong, Y.S., Hoover, J., Jaillon, O., Ke, Z.X., Kodira, C., Kokoza, E., Koutsos, A., Letunic, I., Levitsky, A., Liang, Y., Lin, J.J., Lobo, N.F., Lopez, J.R., Malek, J.A., McIntosh, T.C., Meister, S., Miller, J., Mobarry, C., Mongin, E., Murphy, S.D., O'Brochta, D.A., Pfannkoch, C., Qi, R., Regier, M.A., Remington, K., Shao, H.G., Sharakhova, M.V., Sitter, C.D., Shetty, J., Smith, T.J., Strong, R., Sun, J.T., Thomasova, D., Ton, L.Q., Topalis, P., Tu, Z.J., Unger, M.F., Walenz, B., Wang, A.H., Wang, J., Wang, M., Wang, X.L., Woodford, K.J., Wortman, J.R., Wu, M., Yao, A., Zdobnov, E.M., Zhang, H.Y., Zhao, Q., Zhao, S.Y., Zhu, S.P.C., Zhimulev, I., Coluzzi, M., della Torre, A., Roth, C.W., Louis, C., Kalush, F., Mural, R.J., Myers, E.W., Adams, M.D., Smith, H.O., Broder, S., Gardner, M.J., Fraser, C.M., Birney, E., Bork, P., Brey, P.T., Venter, J.C., Weissenbach, J., Kafatos, F.C., Collins, F.H., Hoffman, S.L., 2002. The genome sequence of the malaria mosquito Anopheles gambiae. Science 298, 129-+.

Ignarro, L.J., Ballot, B., Wood, K., 1984. Regulation of soluble guanylate cyclase activity by porphyrins and metalloporphyrins. Journal of Biological Chemistry 259, 6201-6207.

Klemz, R., Reischl, S., Wallach, T., Witte, N., Jürchott, K., Klemz, S., Lang, V., Lorenzen, S., Knauer, M., Heidenreich, S., 2017. Reciprocal regulation of carbon monoxide metabolism and the circadian clock. Nature Structural and Molecular Biology 24, 15.

Lara, F., Lins, U., Bechara, G., Oliveira, P., 2005. Tracing heme in a living cell: hemoglobin degradation and heme traffic in digest cells of the cattle tick Boophilus microplus. Journal of Experimental Biology 208, 3093-3101.

457 Lian, L.-Y., Widdowson, P., McLaughlin, L.A., Paine, M.J.I., 2011. Biochemical Comparison of
458 *Anopheles gambiae* and Human NADPH P450 Reductases Reveals Different 2′-5′-ADP and FMN
459 Binding Traits. PLoS ONE 6, e20574.
460 Maines, M.D., 1981. Zinc protoporphyrin is a selective inhibitor of heme oxygenase activity in the
461 neonatal rat. Biochimica Et Biophysica Acta 673, 339-350.
462 Marinotti, O., Nguyen, Q.K., Calvo, E., James, A.A., Ribeiro, J.M.C., 2005. Microarray analysis of genes
463 showing variable expression following a blood meal in Anopheles gambiae. Insect Molecular Biology 14,
464 365-373.
465 Maya-Monteiro, C.M., Daffre, S., Logullo, C., Lara, F.A., Alves, E.W., Capurro, M.L., Zingali, R.,
466 Almeida, I.C., Oliveira, P.L., 2000. HeLp, a heme lipoprotein from the hemolymph of the cattle tick,
467 Boophilus microplus. Journal of Biological Chemistry 275, 36584-36589.
468 Muramoto, T., Kohchi, T., Yokota, A., Hwang, I., Goodman, H.M., 1999. The Arabidopsis
469 Photomorphogenic Mutant *hy1* Is Deficient in Phytochrome Chromophore Biosynthesis as a Result of a
470 Mutation in a Plastid Heme Oxygenase. The Plant Cell 11, 335-347.
471 Němeček, D., Dvořáková, M., Sedmíková, M., 2017. Heme oxygenase/carbon monoxide in the female
472 reproductive system: an overlooked signalling pathway. International journal of biochemistry and
473 molecular biology 8, 1.
474 Ngufor, C., N'Guessan, R., Fagbohoun, J., Odjo, A., Malone, D., Akogbeto, M., Rowland, M., 2014.
475 Olyset Duo®(a pyriproxyfen and permethrin mixture net): an experimental hut trial against pyrethroid
476 resistant Anopheles gambiae and Culex quinquefasciatus in Southern Benin. PLoS One 9, e93603.
477 Notredame, C., Higgins, D.G., Heringa, J., 2000. T-Coffee: A novel method for fast and accurate multiple
478 sequence alignment. Journal of molecular biology 302, 205-217.
479 Oliveira, M.F., Kycia, S.W., Gomez, A., Kosar, A.J., Bohle, D.S., Hempelmann, E., Menezes, D.,
480 Vannier-Santos, M.A., Oliveira, P.L., Ferreira, S.T., 2005. Structural and morphological characterization
481 of hemozoin produced by Schistosoma mansoni and Rhodnius prolixus. Febs letters 579, 6010-6016.
482 Oliveira, M.F., Silva, J.R., Dansa-Petretski, M., de Souza, W., Lins, U., Braga, C.M.S., Masuda, H.,
483 Oliveira, P.L., 1999. Haem detoxification by an insect. Nature 400, 517-518.

484 Oliveira, P.L., Kawooya, J.K., Ribeiro, J.M.C., Meyer, T., Poorman, R., Alves, E.W., Walker, F.A.,
485 Machado, E.A., Nussenzveig, R.H., Padovan, G.J., Masuda, H., 1995. A heme-binding protein from
486 hemolymph and oocytes of the bloodsucking insect, Rhodnius prolixus - isolation and characterisation.
487 Journal of Biological Chemistry 270, 10897-10901.
488 Otterbein, L.E., Bach, F.H., Alam, J., Soares, M., Tao Lu, H., Wysk, M., Davis, R.J., Flavell, R.A., Choi,
489 A.M., 2000. Carbon monoxide has anti-inflammatory effects involving the mitogen-activated protein
490 kinase pathway. Nature medicine 6.
491 Paes, M.C., Oliveira, M.B., Oliveira, P.L., 2001. Hydrogen peroxide detoxification in the midgut of the
492 blood-sucking insect, Rhodnius prolixus. Archives of Insect Biochemistry and Physiology 48, 63-71.
493 Paiva-Silva, G.O., Cruz-Oliveira, C., Nakayasu, E.S., Maya-Monteiro, C.M., Dunkov, B.C., Masuda, H.,
494 Almeida, I.C., Oliveira, P.L., 2006. A heme-degradation pathway in a blood-sucking insect. Proceedings
495 of the National Academy of Sciences of the United States of America 103, 8030-8035.
496 Pereira, L.O.R., Oliveira, P.L., Almeida, I.C., Paiva-Silva, G.O., 2007. Biglutaminyl-biliverdin IX alpha
497 as a heme degradation product in the dengue fever insect-vector Aedes aegypti. Biochemistry 46, 6822-
498 6829.
499 Ranson, H., Nikou, D., Hutchinson, M., Wang, X., Roth, C.W., Hemingway, J., Collins, F.H., 2002.
500 Molecular analysis of multiple cytochrome P450 genes from the malaria vector, Anopheles gambiae.
501 Insect Molecular Biology 11, 409-418.
502 Schmitt, T.H., Frezzatti, W.A., Schreier, S., 1993. Hemin induced lipid membrane disorder and increased
503 permeability - a molecular model for the mechanism of cell lysis. Archives of Biochemistry and
504 Biophysics 307, 96-103.
505 Schuller, D.J., Wilks, A., de Montellano, P.R.O., Poulos, T.L., 1999. Crystal structure of human heme
506 oxygenase-l. Nature Structural Biology 6, 860-867.
507 Soares, M.P., Usheva, A., Brouard, S., Berberat, P.O., Gunther, L., Tobiasch, E., Bach, F.H., 2002.
508 Modulation of endothelial cell apoptosis by heme oxygenase-1-derived carbon monoxide. Antioxidants
509 and Redox Signaling 4, 321-329.

510 Soldano, A., Yao, H., Rivera, M., Ceccarelli, E.A., Catalano-Dupuy, D.L., 2014. Heme-iron utilization by
511 Leptospira interrogans requires a heme oxygenase and a plastidic-type ferredoxin-NADP+ reductase.
512 Biochimica et Biophysica Acta (BBA) - General Subjects 1840, 3208-3217.
513 Stec, D.E., Drummond, H.A., Vera, T., 2008. Role of carbon monoxide in blood pressure regulation.
514 Hypertension 51, 597-604.
515 Stevenson, B.J., Bibby, J., Pignatelli, P., Muangnoicharoen, S., O'Neill, P.M., Lian, L.-Y., Müller, P.,
516 Nikou, D., Steven, A., Hemingway, J., 2011. Cytochrome P450 6M2 from the malaria vector Anopheles
517 gambiae metabolizes pyrethroids: sequential metabolism of deltamethrin revealed. Insect biochemistry
518 and molecular biology 41, 492-502.
519 Stocker, R., Yamamoto, Y., McDonagh, A.F., Glazer, A.N., Ames, B.N., 1987. Bilirubin is an antioxidant
520 of possible physiological importance. Science 235, 1043-1047.
521 Tappel, A.L., 1955. Unsaturated lipid oxidation catalyzed by hematin compounds. Journal of Biological
522 Chemistry 217, 721-733.
523 Tenhunen, R., Marver, H.S., Schmid, R., 1968. Enzymatic conversion of heme to bilirubin by microsomal
524 heme oxygenase. Proceedings of the National Academy of Sciences of the United States of America 61,
525 748-&.
526 Tijet, N., Helvig, C., Feyereisen, R., 2001. The cytochrome P450 gene superfamily in Drosophila
527 melanogaster: Annotation, intron-exon organization and phylogeny. Gene 262, 189-198.
528 Toh, S.Q., Glanfield, A., Gobert, G.N., Jones, M.K., 2010. Heme and blood-feeding parasites: friends or
529 foes? Parasites & vectors 3, 108.
530 Walter-Nuno, A.B., Taracena, M.O., Mesquita, R.D., Oliveira, P.L., Paiva-Silva, G.D.O., 2018. Silencing
531 of Iron and Heme-Related Genes Revealed a Paramount Role of Iron in the Physiology of the
532 Hematophagour Vector *Rhodnius prolixus*. Frontiers in Genetics 9, 19.
533 Wang, M., Roberts, D.L., Paschke, R., Shea, T.M., Masters, B.S.S., Kim, J.-J.P., 1997. Three-dimensional
534 structure of NADPH–cytochrome P450 reductase: Prototype for FMN- and FAD-containing enzymes.
535 Proceedings of the National Academy of Sciences 94, 8411-8416.
536 WHO, 2015. World Health Organisation Fact Sheet 94 - Malaria.

Wilks, A., Black, S.M., Miller, W.L., Ortiz de Montellano, P.R., 1995. Expression and characterization of truncated human heme oxygenase (hHO-1) and a fusion protein of hHO-1 with human cytochrome P450 reductase. Biochemistry 34, 4421-4427.

Wilks, A., de Montellano, P.O., 1993. Rat liver heme oxygenase. High level expression of a truncated soluble form and nature of the meso-hydroxylating species. Journal of Biological Chemistry 268, 22357-22362.

Wilks, A., Ortiz de Montellano, P.R., Sun, J., Loehr, T.M., 1996. Heme oxygenase (HO-1): His-132 stabilizes a distal water ligand and assists catalysis. Biochemistry 35, 930-936.

Wilks, A., Schmitt, M.P., 1998. Expression and Characterization of a Heme Oxygenase (Hmu O) from Corynebacterium diphtheriae - Iron acquisition requires oxidative cleavage of the heme macrocycle. Journal of Biological Chemistry 273, 837-841.

Yuda, M., Hirai, M., Miura, K., Matsumura, H., Ando, K., Chinzei, Y., 1996. cDNA Cloning, Expression and Characterization of Nitric-oxide Synthase from the Salivary Glands of the Blood-Sucking Insect Rhodnius prolixus. European Journal of Biochemistry 242, 807-812.

Zenclussen, M.L., Jensen, F., Rebelo, S., El-Mousleh, T., Casalis, P.A., Zenclussen, A.C., 2012. Heme Oxygenase-1 Expression in the Ovary Dictates a Proper Oocyte Ovulation, Fertilization, and Corpora Lutea Maintenance. American Journal of Reproductive Immunology 67, 376-382.

Zhang, X.H., Sato, M., Sasahara, M., Migita, C.T., Yoshida, T., 2004. Unique features of recombinant heme oxygenase of Drosophila melanogaster compared with those of other heme oxygenases studied. European Journal of Biochemistry 271, 1713-1724.

Zhou, G., Kohlhepp, P., Geiser, D., Frasquillo, M.d.C., Vazquez-Moreno, L., Winzerling, J.J., 2007. Fate of blood meal iron in mosquitoes. Journal of Insect Physiology 53, 1169-1178.

Zhu, W., Wilks, A., Stojiljkovic, I., 2000. Degradation of heme in gram-negative bacteria: the product of the hemO gene of Neisseriae is a heme oxygenase. Journal of bacteriology 182, 6783-6790.

Figure captions

564 **Figure 1. Alignment of putative and confirmed heme oxygenases.** Alignment is constructed
565 with insect (*An. gambiae* (AGAP003975)*, Ae. aegypti* (AAEL008136)*, R. prolixus*
566 (RPRC006832)*, D. melanogaster* (FBgn0037933)), mammalian (*R. norvegicus* (24451)*, H.*
567 *sapiens* HO-1 (3162)) and bacterial (*Corynebacterium diphtheriae* HmuO (AAC44832.1)) heme
568 oxygenases. Areas of high sequence homology are apparent around the proximal and distal
569 sides of the heme binding pocket. Highlighted are conserved residues implicated in distal heme
570 binding (*) and proximal heme binding (‡). Residues implicated in flexing the distal heme
571 binding pocket (°) are divergent in human and insect HOs.
572
573 **Figure 2. Recombinant AgHO.** Lane 1, Molecular mass marker; Lane 2, 0.25µg purified AgHO.
574
575 **Figure 3. UV/visible absorption spectra of various forms of the heme-AgHO complex.**
576 Spectra are shown for different redox states of 10µM AgHO-haem complex.
577
578 **Figure 4. Absorption difference spectra of heme binding to AgHO.** Optical absorption
579 spectra for heme (2-20µM) titrated against AgHO (10µM). Inset is change in absorption at
580 412nm with increasing concentration of heme.
581
582 **Figure 5. Reaction of the heme-AgHO complex with CPR (**A**),** AgCPR; (B**),** MdCPR; (C),
583 HsCPR. Following addition of NADPH, the absorbance of the Soret (398nm) and α/β peaks
584 (603nm, 579nm) decreased with a concomitant increase at 680nm.
585
586 **Figure 6. Difference absorption spectra of the heme-AgHO and CPR reaction in the**
587 **presence of myoglobin**. The reference and sample cuvette contained 10 µM AgHO-heme
588 complex and 3 µM AgCPR. 150 µM myoglobin was added to the sample cuvette, and reactions
589 were initiated with addition of 300 µM NADPH. The shift in Soret peak from 408nm to 414nm
590 was monitored for 30 minutes.

591 **Figure 7. Absorption spectra of the heme-AgHO and CPR reaction in the presence of**
592 **ferrozine**. The sample cuvette contained 10 µM AgHO-heme complex, 3 µM AgCPR and 250
593 µM ferrozine. Reactions were initiated by addition of 300 µM NADPH. Decreased Soret peak
594 absorbance is observed with heme catabolism with increased absorbance at 562nm due to
595 formation of a ferrozine-ferrous iron complex. Inset; increase in absorbance at 562nm due to
596 formation of ferrozine-ferrous iron complex.
597
598 **Figure 8. Effect of pH (A) and temperature (B) on AgHO activity**. The formation of Fe^{2+}-
599 ferrozine complex was used to measure the AgHO reaction rate. Reaction mixtures consisted
600 of 10 µM AgHO-heme complex, 3 µM AgCPR, 250 µM ferrozine in a volume of 200 µL.
601
602 **Figure 9. Zn and Sn protoporphyrins inhibit oviposition in *An. gambiae*.** Adult females
603 were artificially fed human blood supplemented with the concentration of protoporphyrin
604 indicated in the figure. (A) Dose response to ZnPP - One way ANOVA, $F(3,8) = 40.44$, $p < 0.0001$ (B) Dose response to SnPP - One way ANOVA, $F(3,8) = 135.2$, $p < 0.0001$ (C) CuPP
606 does not affect oviposition – unpaired t test, $t(4)=0.68$, $p=0.28$. Data shown are mean +/- SEM,
607 n =3.
608

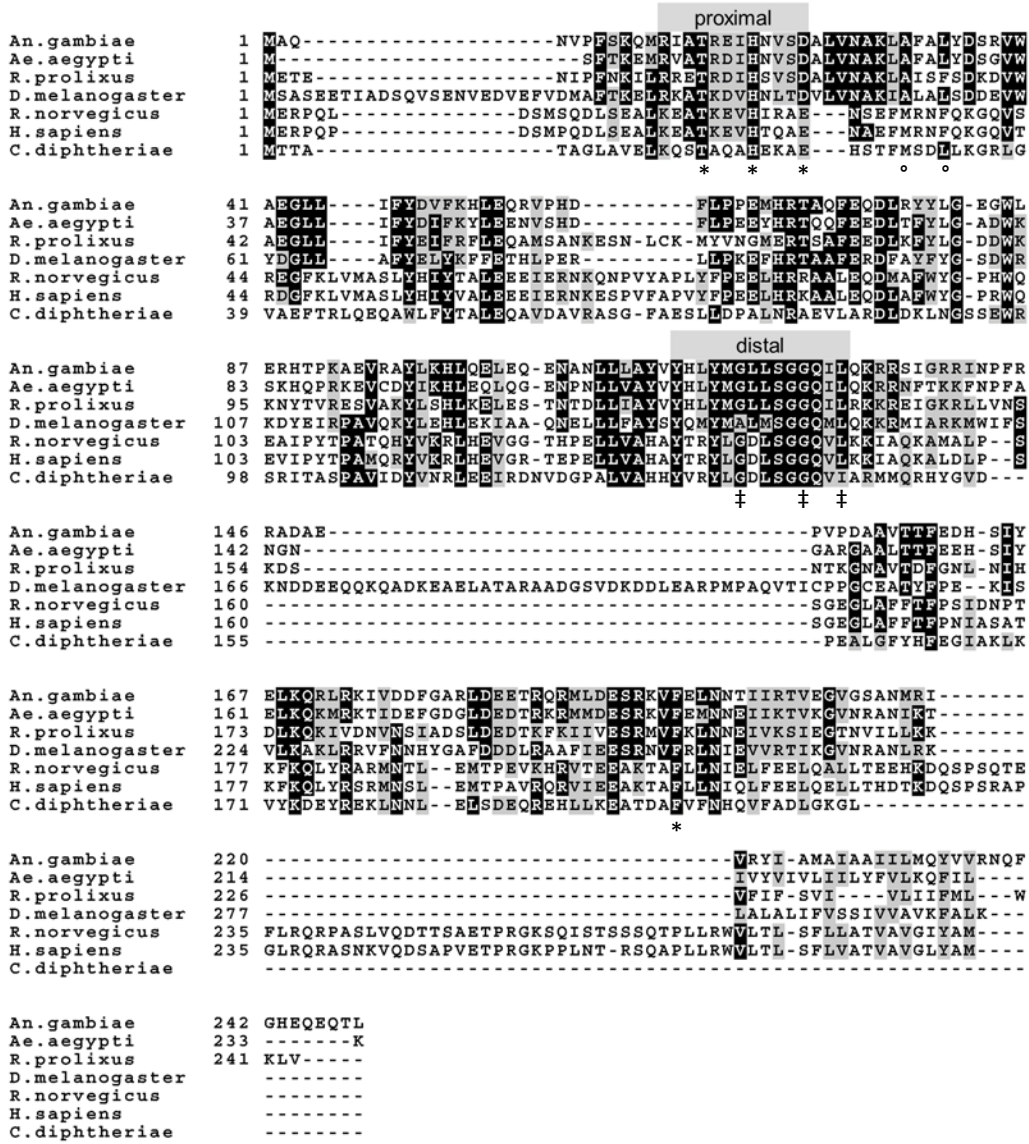
proximal
distal
An.gambiae
Ae.aegypti
R.prolixus
D.melanogaster
R.norvegicus
H.sapiens
C.diphtheriae

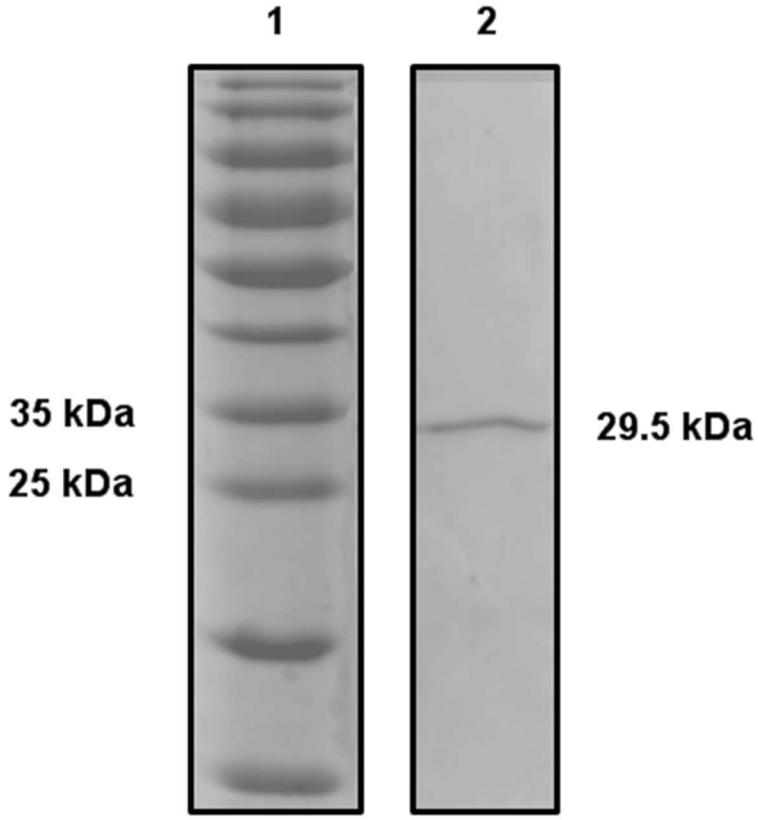

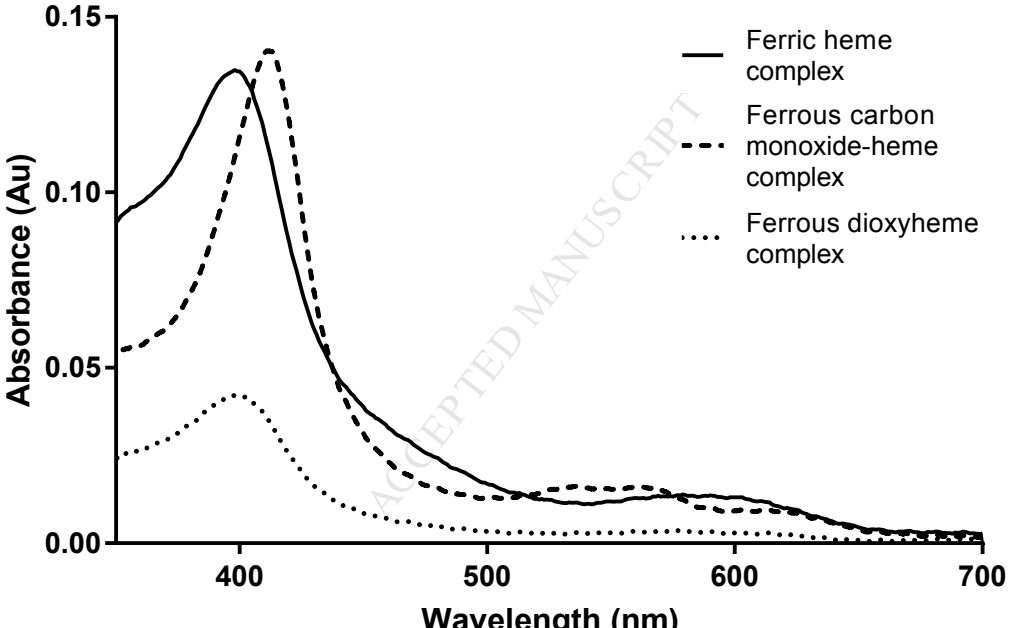

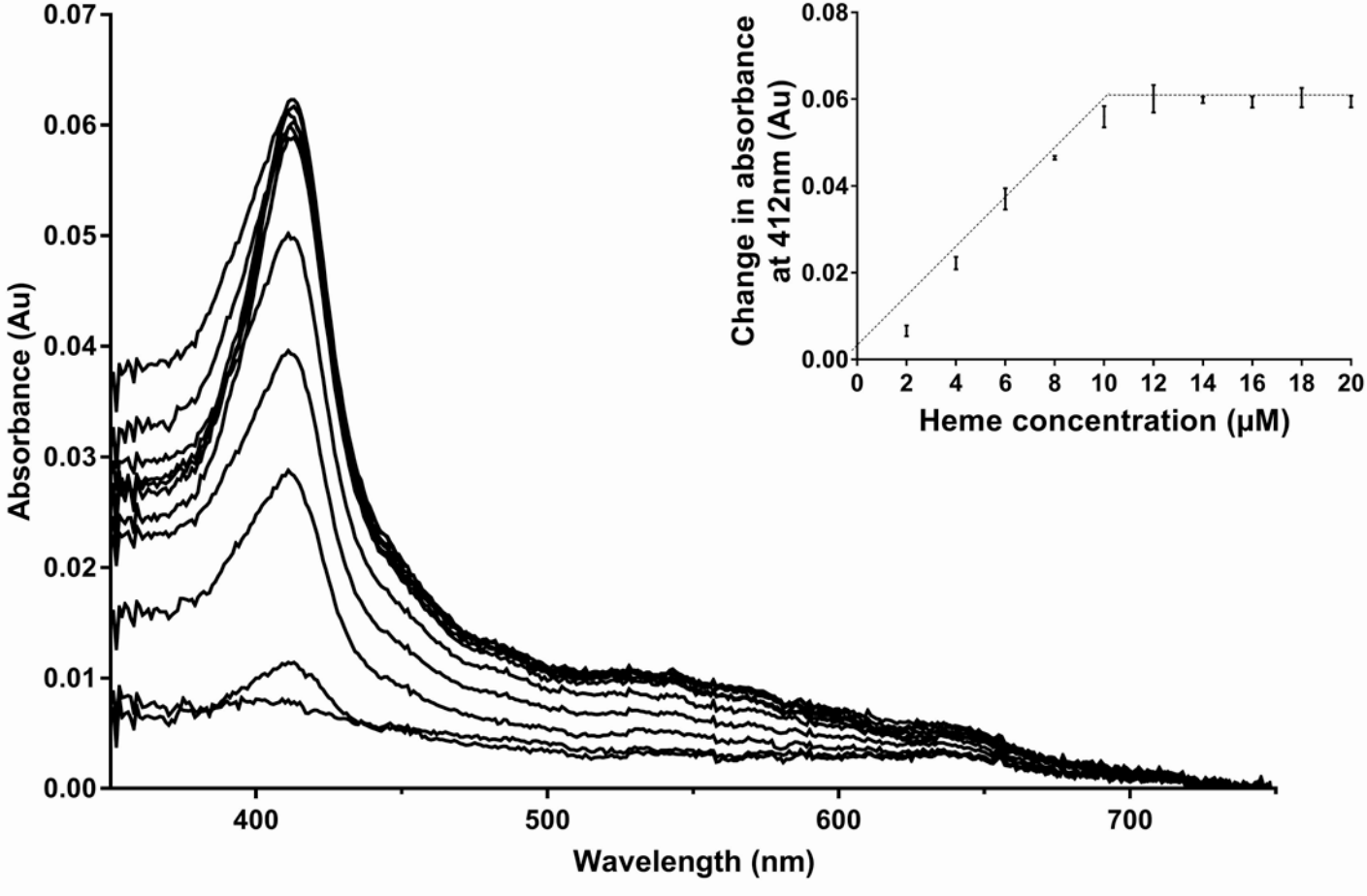
0.07
0.06
0.05
0.04
0.03
0.02
0.01
0.00
Absorbance (Au)
400
500
600
700
Wavelength (nm)
0.08
0.06
0.04
0.02
0.00
Change in absorbance at 412nm (Au)
0
2
4
6
8
10
12
14
16
18
20
Heme concentration (μM)

A

AgCPR

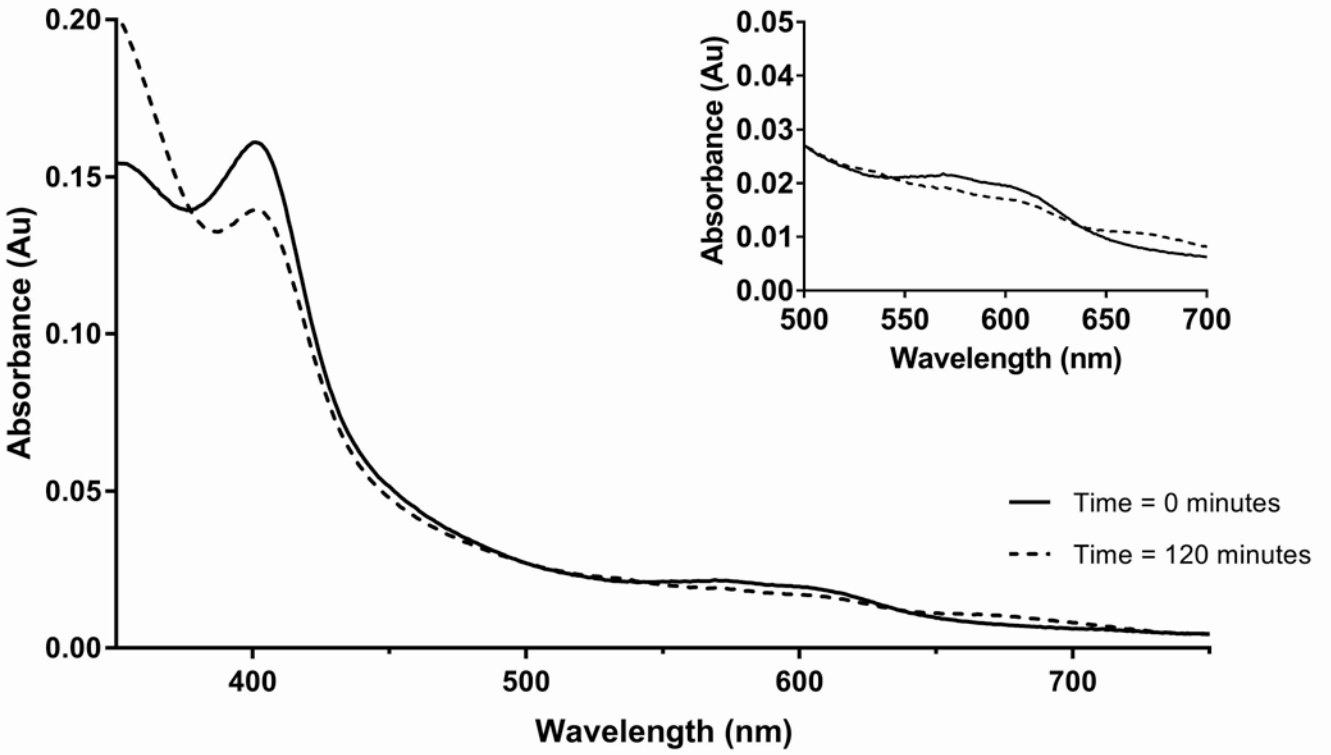

B

MdCPR

C

HsCPR

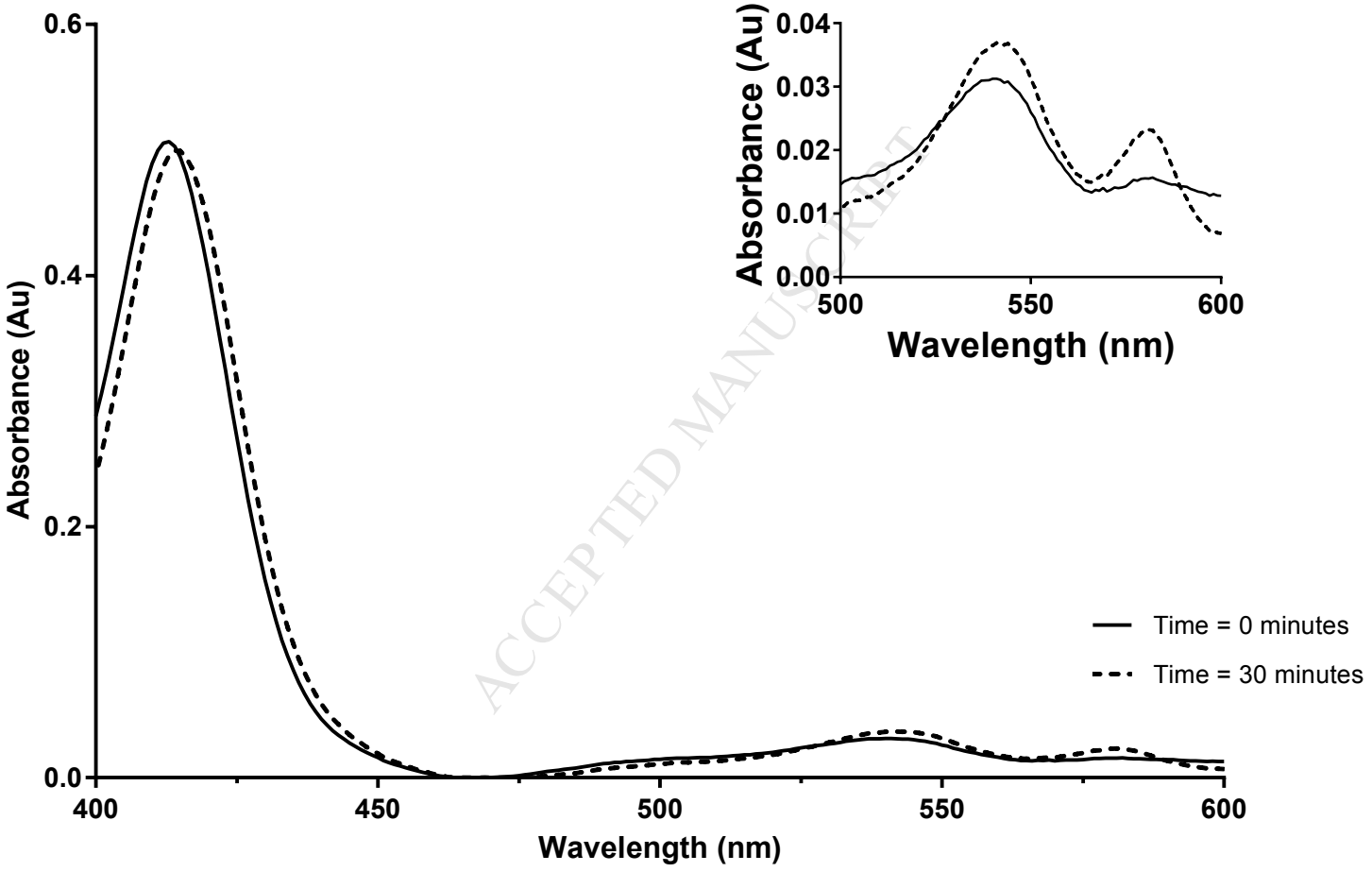

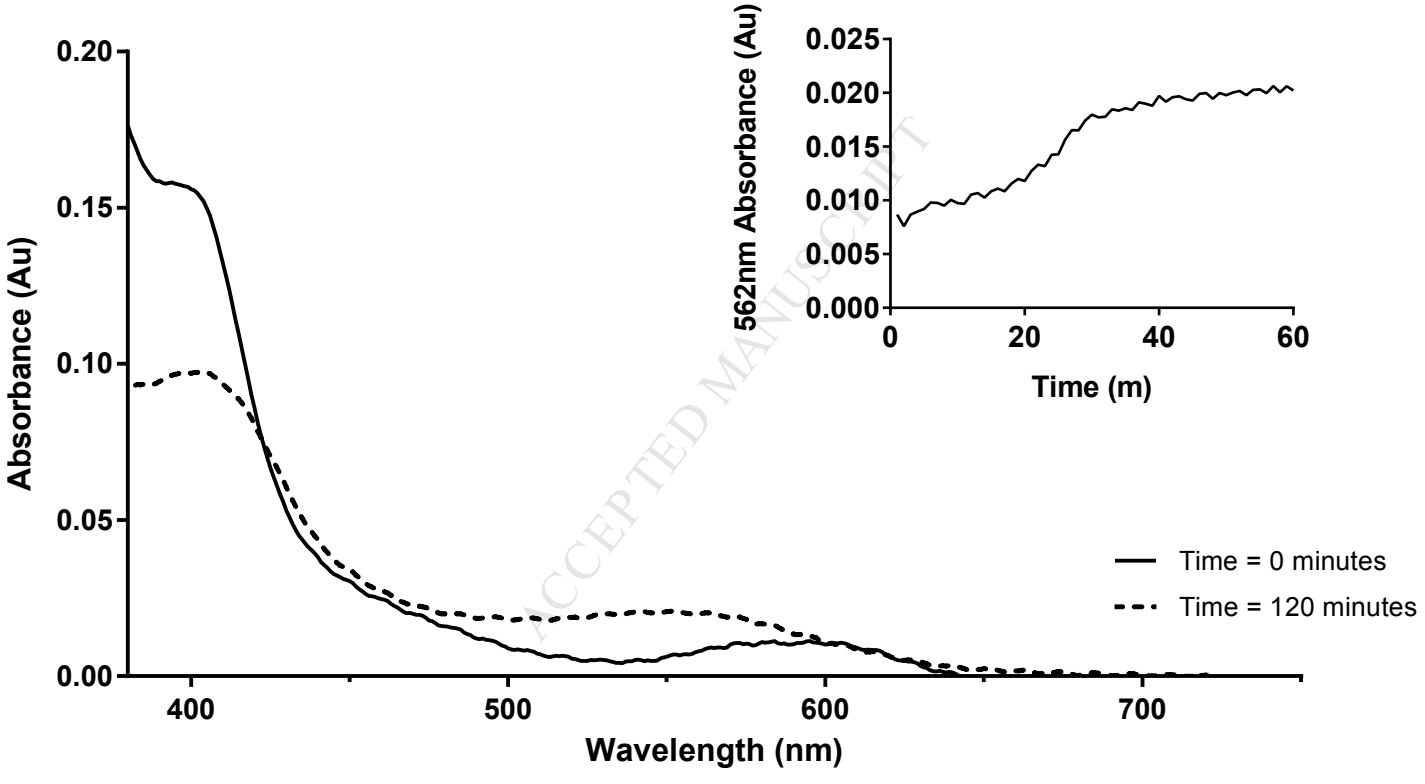

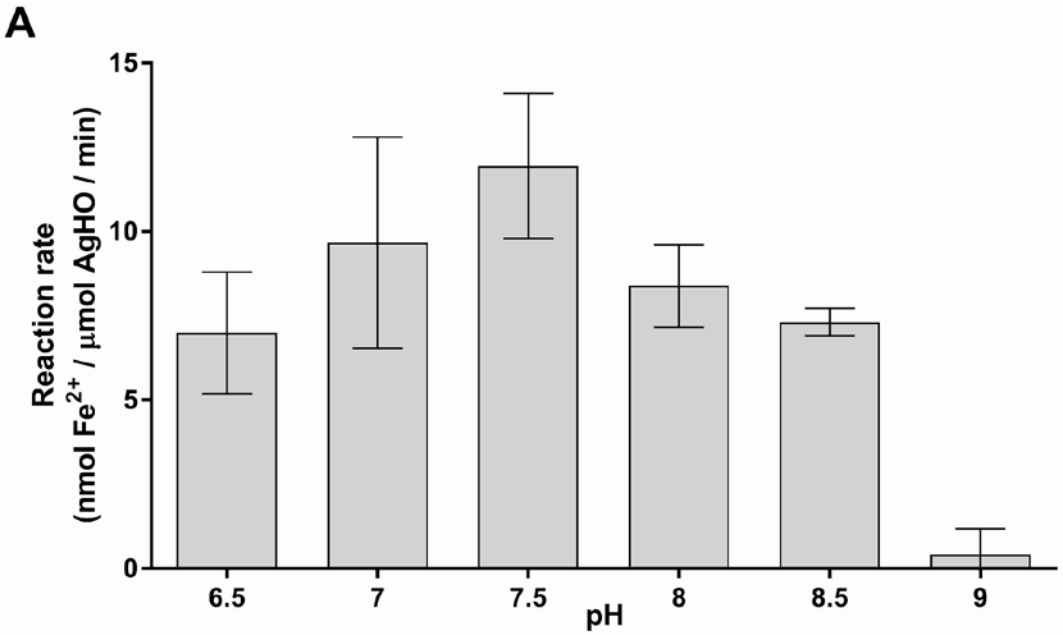
A
Reaction rate
(nmol Fe^{2+} / µmol AgHO / min)
15
10
5
0
6.5
7
7.5
8
8.5
9
pH

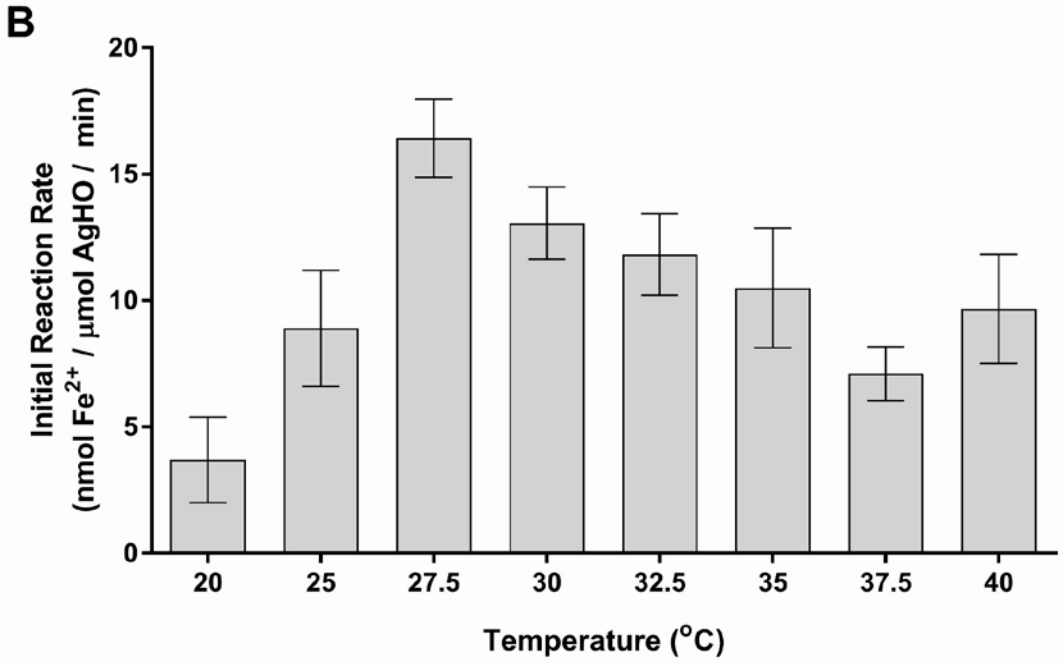
B
Initial Reaction Rate
(nmol Fe^{2+} / µmol AgHO / min)
20
15
10
5
0
20
25
27.5
30
32.5
35
37.5
40
Temperature (^{o}C)

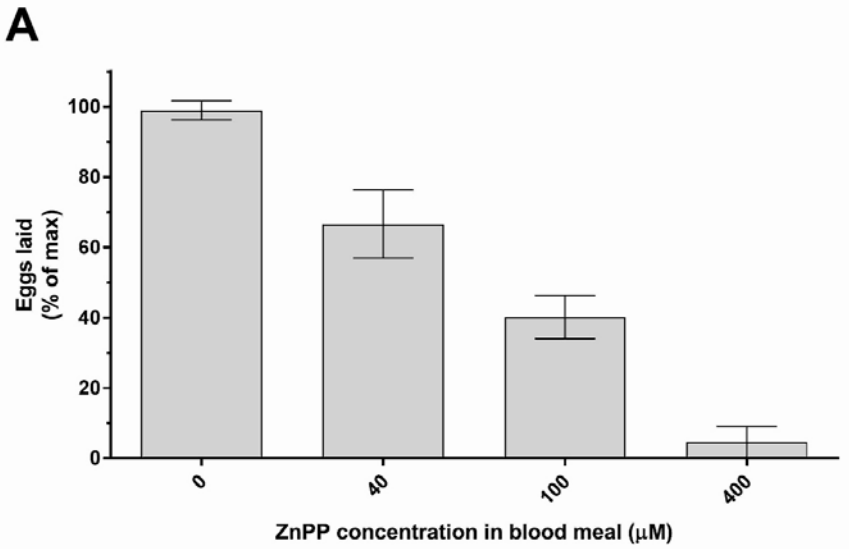
A
Eggs laid
(% of max)
0
20
40
60
80
100
0
40
100
400
ZnPP concentration in blood meal (μM)

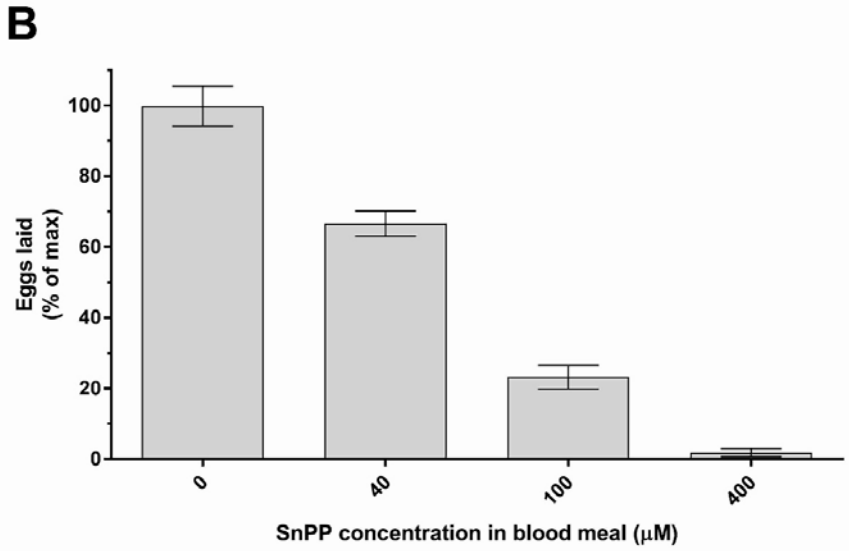
B
Eggs laid
(% of max)
0
20
40
60
80
100
0
40
100
400
SnPP concentration in blood meal (μM)

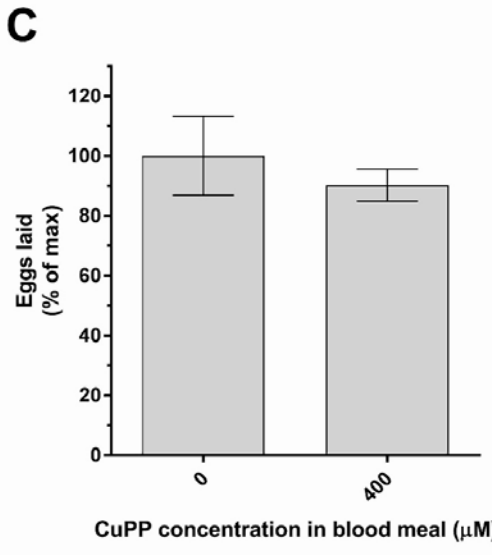
C
Eggs laid
(% of max)
0
20
40
60
80
100
120
0
400
CuPP concentration in blood meal (μM)

Research Highlights

- Recombinant *Anopheles gambiae* HO (AgHO) expressed in *E. coli*
- Purified AgHO binds heme and exhibits heme oxygenase activity
- Inhibition of heme oxygenase activity with Zn- and Sn-protoporphyrin adult *An. gambiae* compromises oviposition
- AgHO presents a potential target for the development of compounds aimed at sterilising mosquitoes for vector control